



A new method for hydroforming of thin-walled spherical parts using overlapping tubular blanks

Cong Han^{1,2} · Hao Feng¹

Received: 26 May 2019 / Accepted: 20 November 2019 / Published online: 19 December 2019
© Springer-Verlag London Ltd., part of Springer Nature 2019

Abstract

Tube hydroforming is an advanced metal forming processes, which is widely used to form various tubular parts. Axial feeding is usually used to avoid excessive thinning in hydroforming of a variable-diameter part. However, wrinkling defects are susceptible to occur easily under the axial loading if the wall thickness of the tube is small. A new method was proposed to enhance the expansion ratio and improve the thickness distribution for hydroforming of thin-walled spherical parts using overlapping tubular blanks. A special loading tool was created and AISI 304 stainless steel blanks were used for the experimental research. The effects of blank shapes and normal constraints were studied on wrinkling defects of the overlapping blanks. The results show that wrinkling defects at the inner layer of the overlap are prevented by using curved-edge blanks. Wrinkling defects at the outer layer of the overlap is eliminated by using normal constraints. Finally, a sound thin-walled spherical part was obtained by using an overlapping tubular blank. The maximum expansion ratio is 60% and increased by 30.2% compared with that of conventional hydroforming using a closed cross-sections tube. The maximum thinning ratio was 32.4%, which was decreased by 29.3%. In general, it is feasible to use an overlapping blank to form a variable diameter part. The maximum expansion enhances significantly and the thickness distribution improves apparently.

Keywords Hydroforming · Overlapping blank · Thin-walled · Wrinkling · Thickness

1 Introduction

Tube hydroforming has been widely studied and applied in aerospace and automotive applications due to its weight reduction, part consolidation, and low cost [1]. Variable diameter tubular components are used for the piping system in aircrafts and rockets as a kind of typical hydroformed parts. The structure characteristic is that the diameter of the middle is larger than that of the end [2]. The expansion ratio and thickness distribution are important indicators to evaluate the hydroformability [3].

In general, the hydroformability of variable diameter tubular components is influenced by material parameters, friction

conditions, loading paths, and so on [4]. Up to now, the influence of material parameters on free-expansion behavior has been adequately studied using analytical model and experimental methods [5]. The experimental results have shown that the wall thickness can be improved when tubular materials with high strain hardening exponent and high plastic anisotropy were selected [6]. Friction between the tube and die plays a key role in hydroforming process [7]. A uniform thickness distribution can be obtained by a lower friction coefficient [8]. Therefore, lubricants were used to decrease the friction coefficient [9]. A good lubrication condition can reduce the thickness differences between bulged and non-bulged regions [10]. Special forming setup has provided another way to enhance the hydroformability. The friction force was reduced, and the thickness distribution was improved by using a movable die [11]. The local strain gradient at potential necking sites was reduced by using a restrictive ring at the bulging zone in bulging of HF440 tubes [12]. In addition, the forming limit can be also enhanced by changing the deformation mode. An integrated-type axle-housing, which was a tubular part with an expansion nearly as large as 3.0 times the cross-sectional length of the initial blank, was manufactured by pure shear

✉ Cong Han
conghan@hit.edu.cn

¹ School of Materials Science and Engineering, Harbin Institute of Technology, Harbin 150001, China

² National Key Laboratory of Precision Hot Processing of Metals, Harbin Institute of Technology, Harbin 150001, China

deformation [13]. Useful wrinkles, furthermore, have been proved effective to improve the forming limit and thickness distribution in hydroforming of variable diameters tubular components [14]. Basically, useful wrinkles can be obtained by optimizing the loading path [15]. A number of researches on the optimization method of loading paths have been reported [16]. A global sensitivity analysis and multi-objective method based on meta-modeling techniques was used to optimize the loading path [17]. A hybrid-constrained MOGA and local search method was applied, and the maximum thinning was obviously reduced in hydroforming of mild steel DP600 [18].

However, it is difficult to push the material from the guiding area to the bulging area if the axis of the part is long. Besides, wrinkling defects are susceptible to occur easily under the axial loading if the diameter-to-thickness ratio (D/t) of the tube is extremely small. The critical strains for wrinkles will drop sharply with the increasing of D/t [19]. For these cases, therefore, it is not feasible to enhance the forming limit by increasing the axial loading.

In this paper, a new method of using an overlapping tubular blank was put forward to manufacture a thin-walled spherical part. A special loading tool was created, and AISI 304 stainless steel blanks were used for experimental research. In addition, wrinkling defects of the overlapping blanks was studied. The effects of the blank shape and normal constraints on the wrinkling defects were analyzed. On the basis of it, a thin-walled spherical part without forming defects was manufactured successfully. Finally, the comparison of thickness distribution was analyzed between using an overlapping blank and using a tube with closed cross-sections.

2 Sample and material

The sample is a spherical part, as shown in Fig. 1. The radius of the sphere is 60 mm, and the length is 98 mm. The radius of the fillet is 5 mm at the transition areas. The diameter is 76 mm

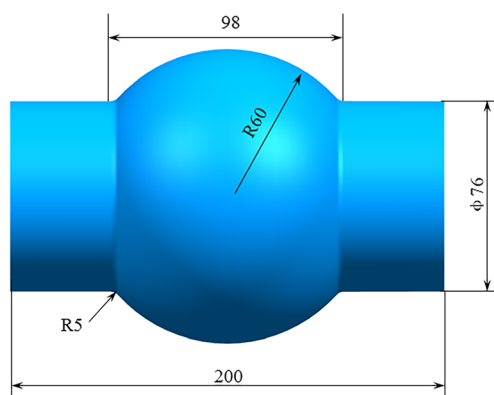


Fig. 1 Shape and dimension of the sample

at both sides of the part. The total length of the sample is 200 mm.

AISI 304 stainless steel tubular blanks were used in the experiments. The initial thickness of the blank was 0.5 mm. Standard specimens were tested on a uniaxial tensile testing machine to obtain mechanical properties. The ultimate tensile strength was obtained from the true stress-strain curve. Yield strength was measured by taking the load at 0.2% strain by offset method. The mechanical properties are given in Table 1.

3 Principle of the hydroforming process

3.1 Manufacture process

Figure 2 shows the main manufacture processes of the sample, including hydroforming of the overlapping blank, cutting, welding, and calibration. First, an overlapping tubular blank deformed into a spherical blank by a self-sealing device filled with pressurized liquid in hydroforming process. Next, the redundant part of the overlapping spherical blank was removed in cutting process. Subsequently, the cut blank was welded to form a spherical blank with closed cross-sections. Finally, a calibration process was carried out, and a spherical part was obtained. Each process will be introduced in detail as follows.

1) Hydroforming of the overlapping blank

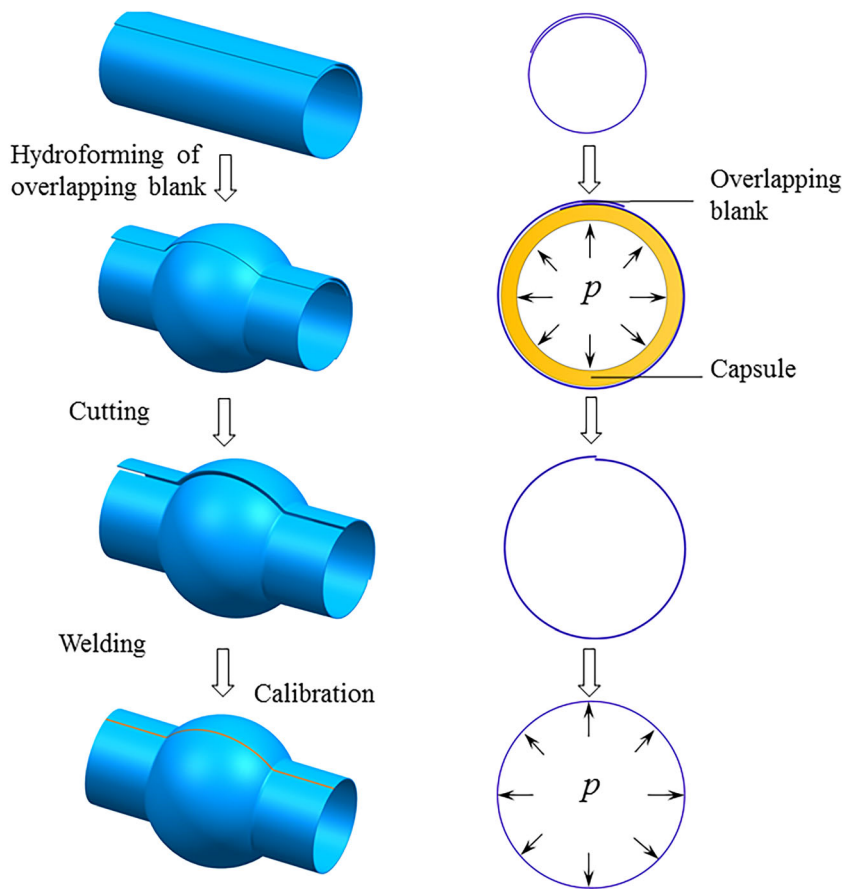
Hydroforming of the overlapping blank is an imperative procedure of the process. The overlapping tubular blank bulged into a spherical blank in this process. The material can flow along the circumferential direction because of the overlapping blank, as shown in Fig. 3. It is difficult to seal the overlapping tubular blank during hydroforming. Therefore, a self-sealing elastic capsule was assembled and inserted into the overlapping tubular blank to realize the seal at the beginning of the process. The upper die and lower die was held together by a hydraulic press. Clamping force was applied to prevent the separation of the die halves. Then the internal pressure of capsule kept increasing until the overlapping blank completely contacted to the die cavity. Finally, the internal pressure was unloaded, and the capsule was taken out from the blank. A spherical overlapping blank was obtained.

2) Cutting

Table 1 Mechanical properties of AISI 304 stainless steel tubular blank

Elastic modulus E (GPa)	Yield strength σ_s (MPa)	Ultimate strength σ_b (MPa)	Elongation δ (%)
204	283	809	52.8

Fig. 2 Manufacture process of the sample



The spherical overlapping blank was cut after hydroforming considering the existence of overlap. The overlap composed of inner and outer layer was cut along the symmetry plane, as shown in Fig. 4. Then the spherical blank trimmed is prepared for welding after the redundant parts at inner layer and outer layer were removed.

3) Welding

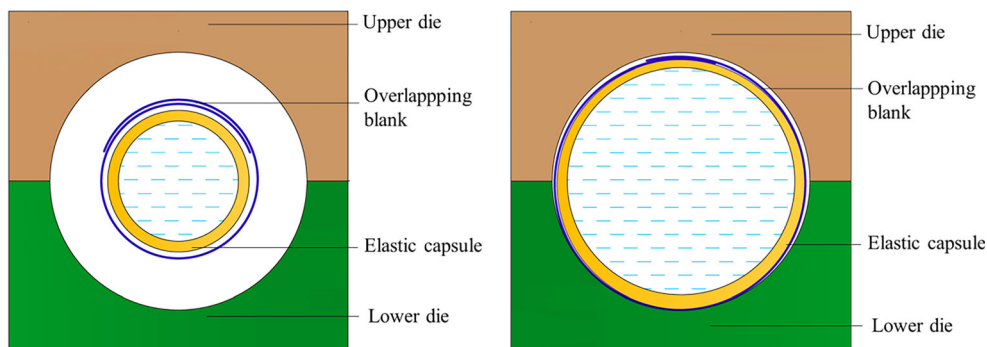
The conjunction of inner and outer layer was realized by argon-arc welding. A spherical tubular blank with closed cross-sections was obtained. Welding deformation may have occurred during welding process. Therefore, the welded

spherical part needs to be hydroformed for calibration to improve the forming precision.

4) Calibration

The calibration of the welded spherical part was conducted with the apparatus used in hydroforming of the overlapping blank. The internal pressure was kept by the elastic capsule. A spherical part was obtained after the blank completely contacted to the die cavity. Thus, the manufacture process of the spherical part was completed.

Fig. 3 Principle of hydroforming of overlapping blank



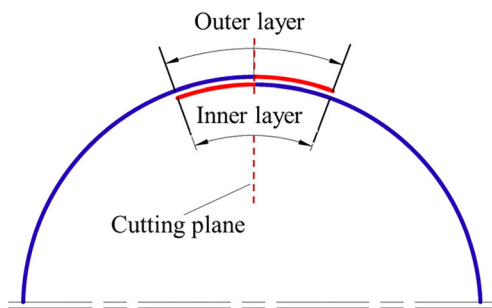


Fig. 4 Location of cutting plane on the spherical blank

3.2 Experimental setup

Figure 5 shows the schematic diagram of the experimental setup for hydroforming of the thin-walled spherical part. The hydroforming tools mainly consist of a lower die, an upper die, and a self-sealing elastic capsule. The shape of die cavity at the middle area was spherical with the radius of 60 mm, and the diameter of die cavity at each end was 76 mm. The self-sealing elastic capsule was filled with pressurized liquid as a loading tool. The overlapping blank deformed as the elastic capsule expanded. A left and right block was assembled to prevent the elastic capsule from stretching along the axial direction.

The experiments were conducted on the 10 MN hydroforming machine. The loading path including the internal pressure and the displacement of punches was input in the control system. The clamping force was applied on the base plate by the hydraulic press before hydroforming process. Emulsion was used as the forming media, and the internal pressure supplied by an intensifier was accurately controlled by the servo hydraulic control valves.

3.3 Research procedure

The overlapping tubular blank was obtained by rolling from a flat sheet with the dimension of 220×340 mm. The diameter and length of the tubular blank was 76 and 220 mm,

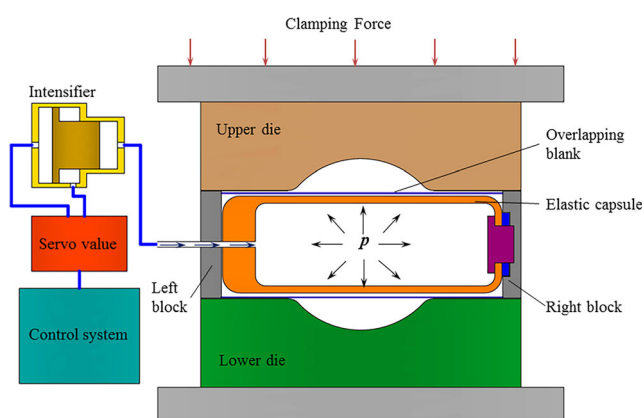


Fig. 5 Schematic diagram of experimental setup

respectively. There was an overlap on the tubular blank, as illustrated in Fig. 4. The maximum forming pressure can be calculated as follows [20]:

$$p_{\max} = \frac{2t}{d} \sigma_b \quad (1)$$

where t and d is the initial wall thickness and the diameter of the blank. σ_b is the ultimate strength, which can be found in Table 1. Accordingly, the calculated maximum forming pressure was 10.64 MPa. In this research, the forming pressure of 10.6 MPa was considered as maximum forming pressure in both hydroforming and calibration processes. The flow of the material along the circumferential direction can be realized by the overlapping blank. Wrinkling defects will occur owing to the difference in the level of the flow of the material at each cross-section, the same as that wrinkle defects occur at the straight side of the flange in square-box drawing. Based on methods to prevent the wrinkling defects in square-box drawing, the effects of blank shapes and normal constraints on wrinkling defects were studied in hydroforming of thin-walled spherical blanks [21].

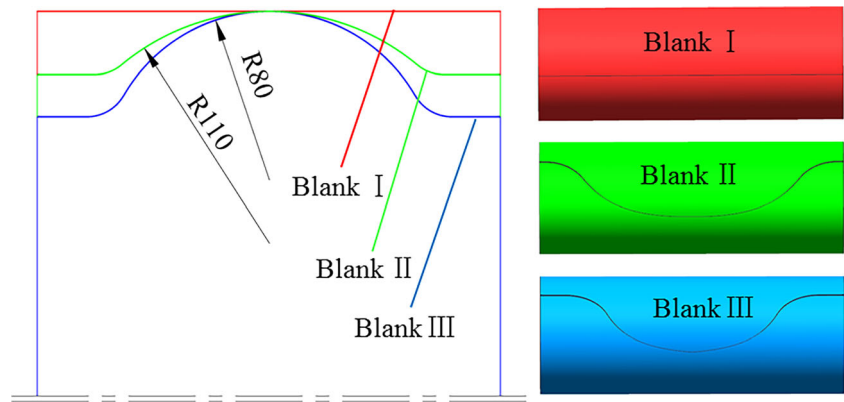
In order to study the effect of blank shapes on wrinkling defects, three shapes of tubular blank were designed, as shown in Fig. 6. The edge shape of blank I was straight. The edge shape of blank II and III was convex. The radius at the edge of blank II and III was 110 mm and 80 mm, respectively. All the maximum perimeters of the cross-section of the three blanks were the same, which were equal to 340 mm.

It has been demonstrated that blank holder force can effectively prevent wrinkling defects in square-box drawing because of the constraint along normal direction [22]. Therefore, normal constraints were used to eliminate the wrinkling defects. A support forced was applied to the blank by the normal constraint during hydroforming of overlapping tubular blanks. Curved plates made of AISI 304 stainless steel was chosen as the normal constraint. The diameter of the curved plate was 76 mm with the central angle of 150 degrees, and the length was 140 mm. The curved plate covered the outer layer of the overlap like a patch, as shown in Fig. 7. The patch plate deformed with the blank and kept supporting the outer layer of the overlap throughout hydroforming process. Two thicknesses of the patch plate were selected as 0.5 and 1.0 mm to study the effect of normal constraints on wrinkling defects.

4 Results and discussion

Wrinkling defects occurred in hydroforming of thin-walled spherical parts using overlapping tubular blanks. However, the wrinkles of the overlap part can be removed in cutting process, which did not influence the forming result in welding and calibration processes. Hence, the cut spherical blank was

Fig. 6 Different shapes of tubular blank



used for the research on wrinkling defects. The effects of blank shapes and normal constraints on wrinkling defects will be studied. Subsequently, the maximum expansion and the thickness distribution of a sound part after calibration will be discussed in this section.

4.1 Effect of blank shapes on wrinkling defects

Figure 8a shows the result of hydroforming using a straight-edge blank. The edge of the blank changed from a straight line to a concave line. A bending deformation occurred at the concave edge of the overlapping blank, which brought about a local axial compressive stress. Accordingly, a wrinkling defect occurred perpendicular to the axial direction. The level of bending deformation weakened if the initial shape of the edge was convex. A method of shape compensation was employed to determine the blank shape used in hydroforming of overlapping tubular blank. Firstly, the profile of the edge of the spherical blank was flattened and depicted after hydroforming, as shown

in Fig. 8b. The height of the profile was denoted by h , which was equal to 50 mm. Then, a convex edge of the blank was created for shape compensation based on the concave edge of the hydroformed spherical blank. According to the height of the curved edge, the shape compensations of the blanks can be classified as a full compensation and a partial compensation. Blank II was the partial-compensation blank, and its height of the curved edge was $0.6 h$. On the other hand, blank III was the full-compensation blank, and its height of the curved edge was h , which was equal to the profile of the spherical blank edge using a straight-edge blank.

Figure 9 shows the effect of blank shapes on wrinkling defects in hydroforming of thin-walled spherical parts using overlapping tubular blanks. Wrinkling defects occurred at both outer and inner layers when blank I was used, as shown in Fig. 9a. Wrinkling defects were eliminated at the inner layer by using curved edges of blank II and III, but not at the outer layer, as shown in Fig. 9b and c. In addition, the level of wrinkle at the outer layer of blank II was more severe than that of blank III. This indicates that wrinkling defects can be restrained by increasing the curvature of the blank edge. In general, wrinkling defects are influenced by the local stress state. Therefore, the trajectory of principal stress at the wrinkling zone was analyzed next.

Figure 10 shows the trajectory variation of principal stress at the wrinkling zone with different blank shapes. The principle stress σ_1 and σ_3 refer to a circumferential and axial stress component, respectively. The thickness dividing line separates the principal stress plane into thinning and thickness areas. The material at the wrinkling zone of the outer layer was subjected to a circumferential tensile stress and an axial compressive stress in hydroforming of these blanks with different shapes. There was little influence of blank shape on the circumferential tensile stress. However, the axial compressive stress decreased as the curvature of the blank edge increased. The maximum axial compressive stress of blanks I, II, and III were 645, 595 and 498 MPa, respectively. The axial compressive stress decreased by 147 MPa when the shape of blank edge changed from a straight line to a curve with the radius of

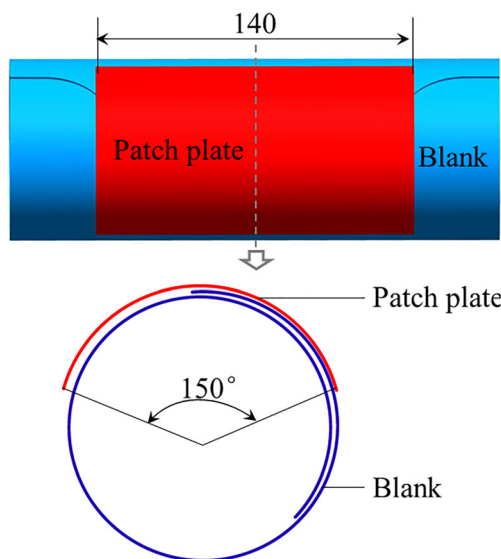


Fig. 7 Schematic view of hydroforming with normal constraints

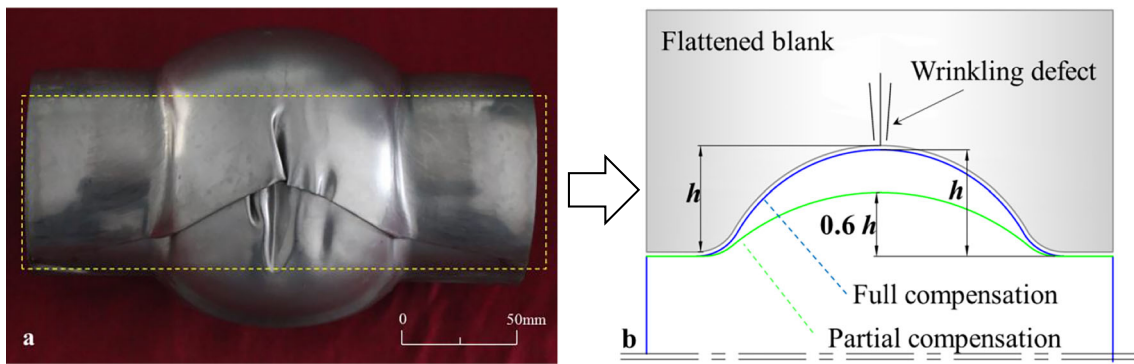


Fig. 8 a Result of hydroforming using a straight-edge blank; b schematic diagram of method of shape compensation of the tubular blank

80 mm. Therefore, a curved shape had a beneficial influence on control of wrinkling defects by reducing the axial compressive stress at the wrinkling zone.

The same as that of the outer layer, the material at the wrinkling zone of the inner layer was subjected to a circumferential tensile stress and an axial compressive stress during hydroforming. Blank shapes had little effect on the

circumferential tensile stress. The reduction of the axial compressive stress was more significant at the inner layer than that at the outer layer when the curvature of the blank edge increased. The maximum axial compressive stress of blanks I, II, and III were 570, 217 and 192 MPa, respectively. The axial compressive stress decreased by 378 MPa when the shape of blank edge changed from a straight line to a curve with the radius of 80 mm. Therefore, a curved shape had a strong effect on the control of wrinkling defects at the inner layer. The axial compressive stress was smaller than the circumferential tensile stress, which brought about a thinning at the inner layer of the blank.

As stated above, wrinkling defects at the inner and outer layer were controlled most effectively by using blank III among the three blanks. Therefore, blank III was used as the

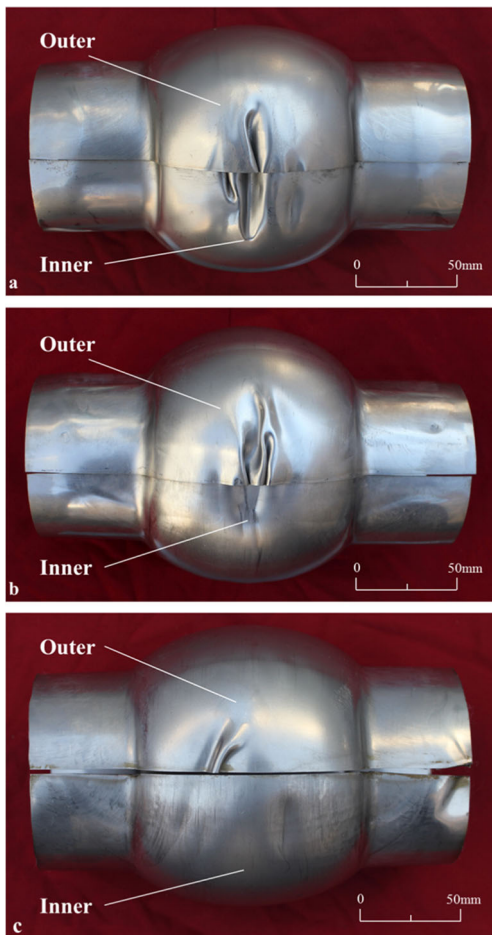


Fig. 9 Effect of blank shapes on wrinkling defects. a. Blank I; b. Blank II; c. Blank III

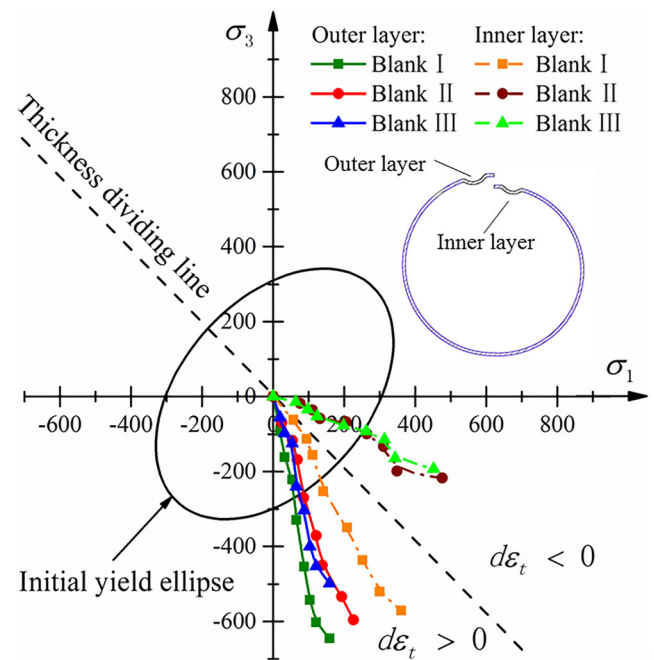


Fig. 10 Trajectory variation of principal stress with different blank shapes at wrinkling zone

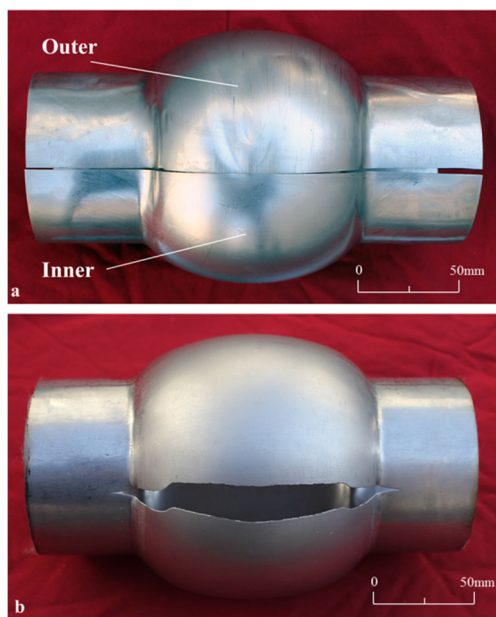


Fig. 11 Effect of normal constraints on formability. a. Elimination of wrinkling defects by using normal constraints; b. Fracture opposite the outer layer using a patch plate with the thickness of 1.0 mm

initial blank to investigate the effect of normal constraints on wrinkling defects.

4.2 Effect of normal constraints on wrinkling defects

Figure 11 shows the effect of normal constraints on wrinkling defects in hydroforming of thin-walled spherical parts using

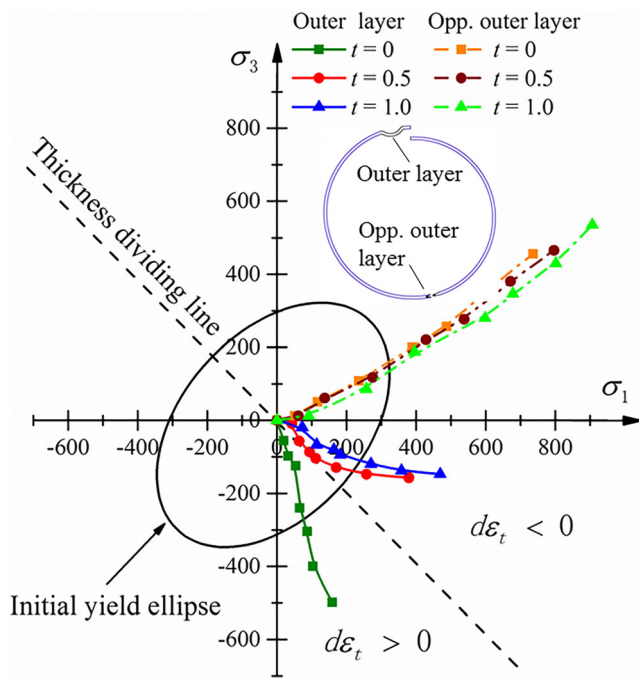


Fig. 12 Trajectory variation of principal stress with different normal constraints at and opposite the wrinkling zone

blank III. Patch plates with different thicknesses were used as the normal constraints. The radius of the curved edge of the blank was 80 mm. The wrinkling defect only appeared at the outer layer because of using blank with a curved edge. The results show that the wrinkle was completely eliminated when the thickness of the patch plate was 0.5 or 1.0 mm, as shown in Fig. 11a. Therefore, a spherical blank free of wrinkling defects was obtained by using a normal constraint and a curved-edge blank. A fracture, however, occurred opposite the outer layer of the spherical blank when the thickness of the patch plate was 1.0 mm, as shown in Fig. 11b. The trajectory of principal stress at and opposite the outer layer was analyzed to investigate the reasons for the elimination of wrinkling defect and the occurrence of bursting.

Figure 12 shows the trajectory variation of principal stress at and opposite the wrinkling zone with different thicknesses of normal constraints. A sharp reduction of axial compressive stress can be seen as normal constraints were applied. The axial compressive stress decreased to 157 and 147 MPa when the thicknesses of the patch plate were 0.5 and 1.0 mm. The tendency of axial compressive stress variation was similar to that at the wrinkling zone of the inner layer, as discussed in Section 4.1. It could be assumed that the outer layer of the blank could be considered as a normal constraint to the inner layer. A thinning at the outer layer may occur as the trajectory of principal stress was above the thickness dividing line.

The stress state opposite the wrinkling zone was also been analyzed to investigate the bursting. A common characteristic was that the material opposite the wrinkling zone was subjected to biaxial tensile stresses. Both circumferential and axial stresses increased with the normal constraint thickening. The stresses opposite the wrinkling zone were 733 and 452 MPa when there was no normal constraint on the blank. And the stresses were 796 and 466 MPa when a normal constraint with the thickness of 0.5 mm was applied. The equivalent stress can be defined as follows:

$$\bar{\sigma} = \frac{1}{\sqrt{2}} \sqrt{(\sigma_1 - \sigma_2)^2 + (\sigma_2 - \sigma_3)^2 + (\sigma_3 - \sigma_1)^2} \quad (2)$$

In this research, the principle stress σ_2 was omitted, and σ_1 and σ_3 meant the circumferential and the axial stress.

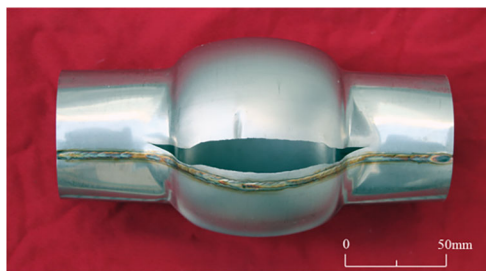


Fig. 13 Hydroformed part using tube with closed cross-sections

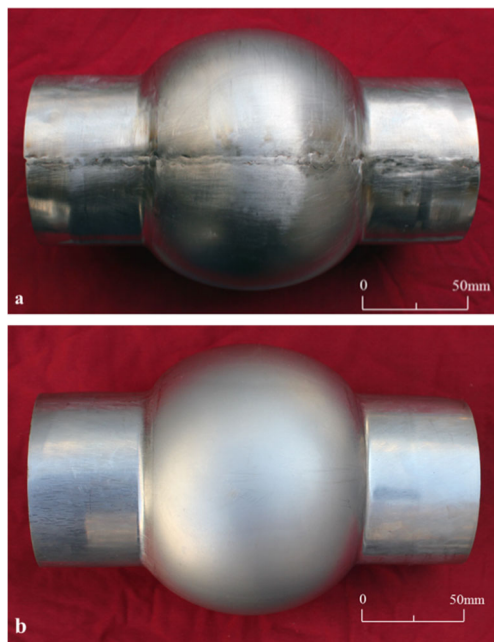


Fig. 14 Spherical parts using overlapping tubular blanks after welding and calibration: **a** at the weld seam; **b** opposite the weld seam

According to Eq. (2), the measured equivalent stresses were 640 and 693 MPa in the cases above. However, the stresses were 907 and 537 MPa when the thickness of the normal constraint was 1.0 mm. The equivalent stress was 790 MPa, which was close to the ultimate strength of 809 MPa. Therefore, a fracture happened opposite the outer layer owing to the excessive circumferential and axial tensile stresses. Based on the effect of normal constraints on the principle stress at and opposite the outer layer, there exists an optimal thickness of normal constraint that can not only eliminate wrinkling defects but also avoid the occurrence of bursting.

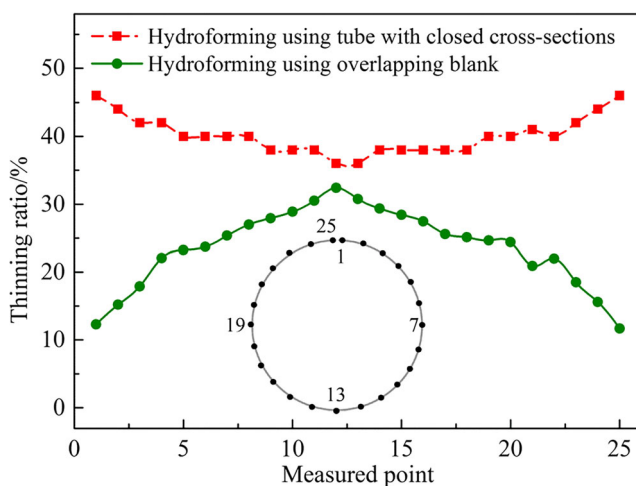


Fig. 15 Comparison of thinning ratio at middle cross-section

4.3 Comparison of maximum expansion

Figure 13 shows the hydroformed part obtained from the conventional hydroforming process by using a tube with closed cross-sections. The diameter of the AISI 304 stainless steel tube was 75.4 mm, and the initial thickness was 0.5 mm. Both ends of the tube were free in the axial direction to make the material flow from each end toward the bulging area. A bursting happened when the maximum expansion of the spherical tube was 46.1%. The maximum expansion can be defined as follows:

$$\eta = \frac{d_{\max} - d}{d} \times 100\% \quad (3)$$

where d_{\max} is the maximum diameter of the part, and d is the initial diameter of the blank.

An appropriate blank shape and normal constraint contributed to avoiding the occurrence of forming defects, as discussed in Section 4.1 and 4.2. Therefore, blank III and a patch plate in thickness of 0.5 mm was used for

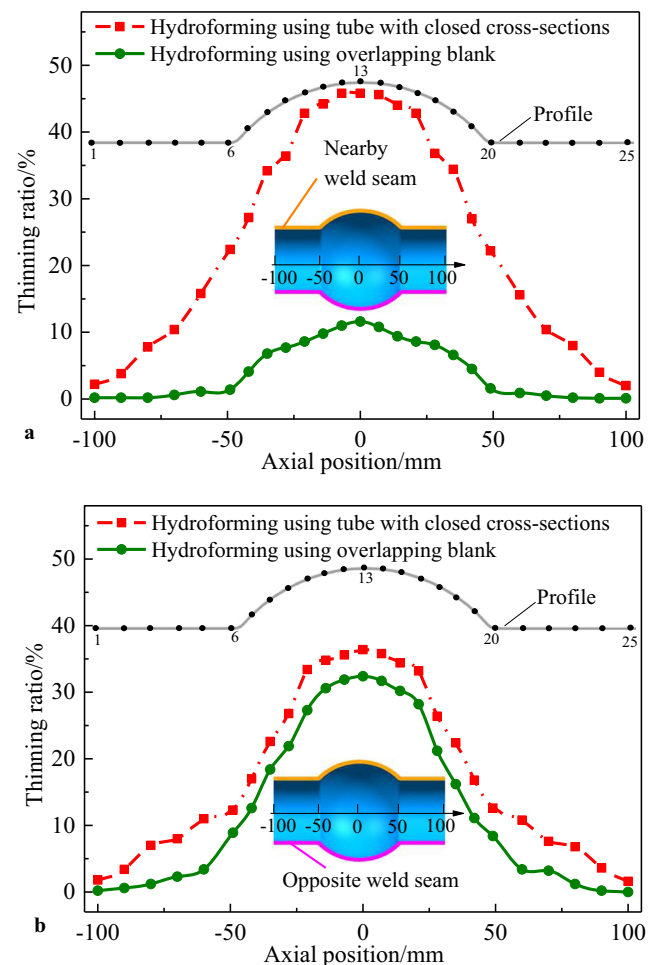


Fig. 16 Comparison of thinning ratio along axial direction: **a** Nearby weld seam; **b** opposite weld seam

hydroforming of the overlapping spherical blank. Then the cut spherical blank was obtained, as shown in Fig. 11a. Finally, a thin-walled spherical part without forming defects was manufactured after welding and calibration, as shown in Fig. 14. The maximum expansion of the thin-walled spherical part reached 60.0%, which increased by 30.2% compared with that in conventional hydroforming using tubes with closed cross-sections. This indicates that the maximum expansion significantly enhances by using overlapping tubular blanks.

4.4 Comparison of thickness distribution

In order to investigate the thickness distribution, there were 25 measured points signed at the middle cross-section of the part where the maximum expansion happened. Point 1 and 25 were close to the weld seam, and point 13 was opposite the weld seam. Figure 15 shows the comparison of thinning ratio at the middle cross-section between the two methods of hydroforming. The minimum thinning ratio was 11.6% next to the weld seam, and the maximum thinning ratio was 32.4% opposite the weld seam when the overlapping blank was used. Meanwhile, there was no fracture after the spherical tube contacted to the die cavity completely. On the other hand, the maximum thinning ratio reached 45.8% until a fracture occurred when the tube with closed cross-sections was used. The maximum thinning ratio using an overlapping blank was 29.3% smaller than that in conventional hydroforming. In addition, even the minimum thickness ratio by using the tube was larger than the maximum thinning ratio by using the overlapping blank. It is apparent that thickness distribution effectively improves by using an overlapping blank in hydroforming of thin-walled spherical parts.

Figure 16 shows the comparison of thinning ratio along the axial direction. The improvement of thickness was obvious nearby the weld seam, as shown in Fig. 16a. The maximum thinning ratio obtained by the overlapping blank was about a quarter as large as that by using the tube with closed cross-sections. However, the difference in thickness distribution opposite the weld seam was relatively subtle, as shown in Fig. 16b. The maximum thinning ratio obtained by the overlapping blank was only 8.9% smaller than that by the tube.

The thickness distribution is more non-uniform when the overlapping blank was used, compared with that using a tube with closed cross-sections. It is because that the shape of the overlapping blank is asymmetric, while the shape of the sample is symmetric. The flow of the material along circumferential direction is much easier at the overlap than opposite the overlap during hydroforming. Therefore, the level of plastic deformation is relatively limited thanks to the flow of the

material at the overlap. The main plastic deformation occurs opposite the overlap. It can be noted that a risk of bursting may increase opposite the overlap if the expansion continues to increase.

5 Conclusions

A new method for hydroforming of thin-walled spherical parts using an overlapping tubular blank was put forward. In addition, the wrinkling defects of the overlapping blanks were studied. The effects of the blank shapes and normal constraints on wrinkling defects were analyzed. A sound thin-walled spherical part with an expansion of 60.0% was manufactured. The improvement of thickness distributions was validated with experimental results. The detailed results were as follows:

- (1) Wrinkling defects at the edge of the overlapping blank were caused by a bending deformation in hydroforming of thin-walled spherical parts. The axial compressive stress continuously increased as the overlapping blank expanded.
- (2) Wrinkling defects at the inner layer of the overlap were prevented by a curved-edge blank. The axial compressive stress at the inner layer obviously decreased when the radius of the overlapping blank edge was 80 mm.
- (3) Wrinkling defects were completely eliminated by using a patch plate as a normal constraint. The axial compressive stress at the outer layer of the overlap decreased dramatically. A fracture occurred when the thickness of the patch plate was 1.0 mm.
- (4) The maximum expansion enhanced using the overlapping tubular blanks. A sound spherical part with an expansion of 60.0% was obtained by using a curved-edge blank with the edge radius of 80 mm and a patch plate with the thickness of 0.5 mm, whereas the maximum expansion was only 46.1% in conventional hydroforming using tubes with closed cross-sections.
- (5) The thickness was effectively improved using the overlapping tubular blanks. The maximum thinning ratio was 32.4%, which was 29.3% smaller than that of conventional hydroforming using tubes with closed cross-sections.

Funding This work was financially supported by the National Natural Science Foundation of China (project number: 51775136). The authors would like to take this opportunity to express their sincere appreciation.

Compliance with ethical standards

Competing interests The authors declare that they have no competing interests.

References

- Koç M, Altan T (2001) An overall review of the tube hydroforming (THF) technology. *J Mater Process Technol* 108(3):384–393
- Yuan SJ, Han C, Wang XS (2006) Hydroforming of automotive structural components with rectangular-sections. *Int J Mach Tools and Manuf* 46(11):1201–1206
- Xie WC, Han C, Chu GN, Yuan SJ (2015) Research on hydro-forming process of closed section tubular parts. *Int J Adv Manuf Technol* 80(5–8):1149–1157
- Alaswad A, Benyounis KY, Olabi AG (2012) Tube hydroforming process: a reference guide. *Mater Des* 33:328–339
- Carleer B, Kevie GVD, Winter LD, Veldhuizen BV (2000) Analysis of the effect of material properties on the hydroforming process of tubes. *J Mater Process Technol* 104(1):158–166
- Manabe KI, Amino M (2002) Effects of process parameters and material properties on deformation process in tube hydroforming. *J Mater Process Technol* 123(2):285–291
- Placak M, Vollertsen F, Woitschig J (2005) Analysis, finite element simulation, and experimental investigation of friction in tube hydroforming. *J Mater Process Technol* 170:220–228
- Ngai G, Jaeger S, Altan T (2004) Lubrication in tube hydroforming (THF): part I. lubrication mechanisms and development of model tests to evaluate lubricants and die coatings in the transition and expansion zones. *J Mater Process Technol* 146(1): 108–115
- Abdelkefi A, Malécot P, Boudeau N, Guermazi N, Haddar N (2017) Evaluation of the friction coefficient in tube hydroforming with the “corner filling test” in a square section die. *Int J Adv Manuf Technol* 88:2265–2273
- Kang BH, Lee MY, Shon SM, Moon YH (2007) Forming various shapes of tubular bellows using a single-step hydroforming process. *J Mater Process Technol* 194(1–3):1–6
- Shin SGR, Joo BD, Tyne CJV, Moon YH (2014) Enhancing tube hydroformability by reducing the local strain gradient at potential necking sites. *J Mech Sci Technol* 28(10):4057–4062
- Zhang Q, Wu CD, Zhao SD (2012) Less loading tube-hydroforming technology on eccentric shaft part by using movable die. *Mater Trans* 53(5):820–825
- Wada M, Mizumura M, Iguchi K, Kaneda H (2014) Large-expansion hydroforming technology achieving three-times expanding. 11th Int Conf Technol Plast (ICTP). Nagoya 81: 2217–2222
- Varma NSP, Narasimhan R (2008) A numerical study of the effect of loading conditions on tubular hydroforming. *J Mater Process Technol* 196(1–3):174–183
- Han C, Liu Q, Lu H, Gao GL, Xie WC, Yuan SJ (2018) Thickness improvement in hydroforming of a variable diameter tubular component by using wrinkles and preforms. *Int J Adv Manuf Technol* 99(9–12):2993–3003
- Imaninejad M, Subhash G, Loukus A (2005) Loading path optimization of tube hydroforming process. *Int J Mach Tools and Manuf* 45(12–13):1504–1514
- Ben Abdesslem A, El-Hami (2014) A global sensitivity analysis and multi-objective optimization of loading path in tube hydroforming process based on metamodelling techniques. *Int J Adv Manuf Technol* 71(5–8):753–773
- An H, Green DE, Johrendt J (2012) A hybrid-constrained MOGA and local search method to optimize the load path for tube hydroforming. *Int J Adv Manuf Technol* 60(9–12):1017–1030
- Paquette JA, Kyriakides S (2006) Plastic buckling of tubes under axial compression and internal pressure. *Int J Mech Sci* 48(8):855–867
- Koç M, Altan T (2002) Prediction of forming limits and parameter in the tube hydroforming process. *Int J Mach Tools and Manuf* 42(1):123–138
- Daxin E, Mizuno T, Li ZG (2008) Stress analysis of rectangular cup drawing. *J Mater Process Technol* 205(1–3):469–476
- S CZ, C GL, L ZQ (2005) Determining the optimum variable blank-holder forces using adaptive response surface methodology (ARSM). *Int J Adv Manuf Technol* 26(1–2):23–29

Publisher's note Springer Nature remains neutral with regard to jurisdictional claims in published maps and institutional affiliations.